Nigerian Journal of Physics (NJP)
ISSN online: 3027-0936
ISSN print: 1595-0611
DOI: https://doi.org/10.62292/njp.v35(s).2026.667
Volume 35(S), 2026

Integrated Aeromagnetic and Radiometric Mapping of Lithological Units in the Nasarawa Basement Complex, North-Central Nigeria

*[1]Musa Yamset Kamal, [1]Olatunji Samuel Ayanninuola, [1]Timbee Terungwa Jacob and [2]Muhammad Sani Isa

[1]Department of Physics, Nasarawa State University, Keffi, Nigeria.
[2]Department of Physics, Yobe State University, Damaturu, Nigeria.

*Corresponding Author's Email: stkamals4us@gmail.com Phone: +2348060932318

Keywords:

Submitted: 23 July 2026

Accepted: 17 Aug. 2026

Published: 16 Sept. 2026

ABSTRACT

This study presents lithological mapping of Nasarawa State, North-Central Nigeria, and using integrated high-resolution aeromagnetic and airborne radiometric data covering about 27,000 km². Aeromagnetic data were processed using Reduction to Equator (RTE), Analytic Signal (AS), First Vertical Derivative (FVD) and Tilt Derivative (TDR), while airborne radiometric data were used to generate potassium (K), thorium (Th), uranium (U), radioelement-ratio and ternary maps. The integrated interpretation delineated the major lithological domains, including migmatite-gneiss complexes, schist belts, granitoids, Younger Granite intrusions, pegmatites, mafic to intermediate intrusive rocks and sedimentary formations of the Middle Benue Trough. The migmatite-gneiss complex generally exhibits moderate to high magnetic responses and low to moderate radioelement concentrations, whereas granitic and Younger Granite bodies show comparatively low to moderate magnetic responses and elevated K, Th and U. Schist belts display variable radiometric responses, reflecting compositional and metamorphic differences, while mafic intrusive rocks are characterised by stronger magnetic responses and generally low radioelement concentrations. Sedimentary formations show low K with moderate Th and U responses. The integrated magnetic-radiometric interpretation provides improved discrimination of lithological boundaries and identifies areas that may warrant further investigation for mineral exploration. The resulting lithological interpretation provides a regional framework for geological mapping and mineral exploration in Nasarawa State, particularly within granitoid, schist, pegmatite and sedimentary terrains.

INTRODUCTION

The Nigerian Basement Complex forms part of the Pan-African mobile belt between the West African and Congo Cratons and records multiple phases of deformation, metamorphism and magmatism (Black, 1980; Dada, 2006; Obaje, 2009). Its lithological diversity is important for understanding mineral occurrence because different rock units and structural settings favour different mineralisation styles. Nasarawa State, in North-Central Nigeria, comprises extensive Basement Complex rocks together with Cretaceous sedimentary successions of the Middle Benue Trough and is recognised for occurrences of lead-zinc, baryte, pegmatite-related rare metals, gemstones and gold (NGSA, 2006; Fatoye et al., 2014). Despite this mineral potential, regional lithological boundaries can be difficult to map where bedrock exposure is limited and weathering is intense. Aeromagnetic and airborne radiometric datasets provide complementary information: magnetic responses are influenced by magnetic susceptibility, lithology and structure, while gamma-ray responses primarily reflect near-surface concentrations of K, Th and U (Dickson & Scott, 1997; Gunn et al., 1997; Shives et al., 2000). Previous aeromagnetic work in Nasarawa State has demonstrated that magnetic anomalies can distinguish basement and sedimentary domains and highlight areas of mineral potential (Adewumi & Salako, 2018). The aim of this study is to delineate lithological units in Nasarawa State using integrated aeromagnetic and airborne radiometric data. Specifically, the study enhances the magnetic data, produces K, Th and U concentration and ratio maps together with a ternary radiometric image, integrates the magnetic and radiometric datasets for lithological discrimination, produces a regional lithological interpretation, and examines the relationship between interpreted lithological domains and known mineral occurrences.

Geological Setting

Regional Geology of Nigeria

The geological setting of Nigeria is composed of three main components, the Basement Complex (Precambrian), Younger Granites (Jurassic) and Sedimentary Basins (Cretaceous to Recent). The Basement Complex is part of the Pan-African mobile belt and has been subjected to at least four major orogenic cycles namely the Liberian (2,700 Ma), the Eburnean (2,000 Ma), the Kibaran (1,100 Ma) and the Pan-African (600 Ma) (Dada, 2006).

The Nigerian Basement Complex is made up of four major petro-lithological units (Obaje, 2009):

i. Migmatite-Gneiss Complex: The basement is mainly composed of migmatites, gneisses, and granite-gneisses.
ii. Schist Belts: Metasedimentary and metavolcanic sequences of phyllites, schists, pelites, quartzites, marbles and amphibolites.
iii. Old Granites: Pan-African granites, granodiorites, syenites, monzonites, gabbros and charnockites.
iv. Acidic and Basic Dykes. Pegmatites with muscovite, tourmaline and beryl: aplites and basaltic/doleritic dykes.

Geology of Nasarawa State

The northern and central parts of Nasarawa State are underlain by the Precambrian Basement Complex formations. These consist of migmatite-gneiss complexes, schist belts and granitoids. The southern and south-eastern parts consist of Cretaceous sedimentary deposits of the Middle Benue Trough (Figure 1). The Benue Trough is split into the Lower, Middle and Upper Benue Trough. The Middle Benue Trough is the area in the southern part of Nasarawa State which is characterised by Cretaceous sedimentary deposits such as Bida Formation, Lafia Formation and Keana/Awe Formation. The trough harbours lead-zinc-barytes mineral deposits that are associated with fractures and shear zones (Fatoye et al., 2014).

Mineralization in the Study Area

Nasarawa State contains documented occurrences of lead-zinc-baryte mineralisation in the Middle Benue Trough and pegmatite- and granite-associated occurrences of lithium, columbite-tantalite and gemstones within the Basement Complex (NGSA, 2006; Fatoye et al., 2014). Gold occurrences are also reported from basement terrains. These occurrences are used in this study as contextual information for interpreting the lithological and structural environments identified from the geophysical datasets; the airborne data are not treated as direct measurements of mineral grade or economic significance.

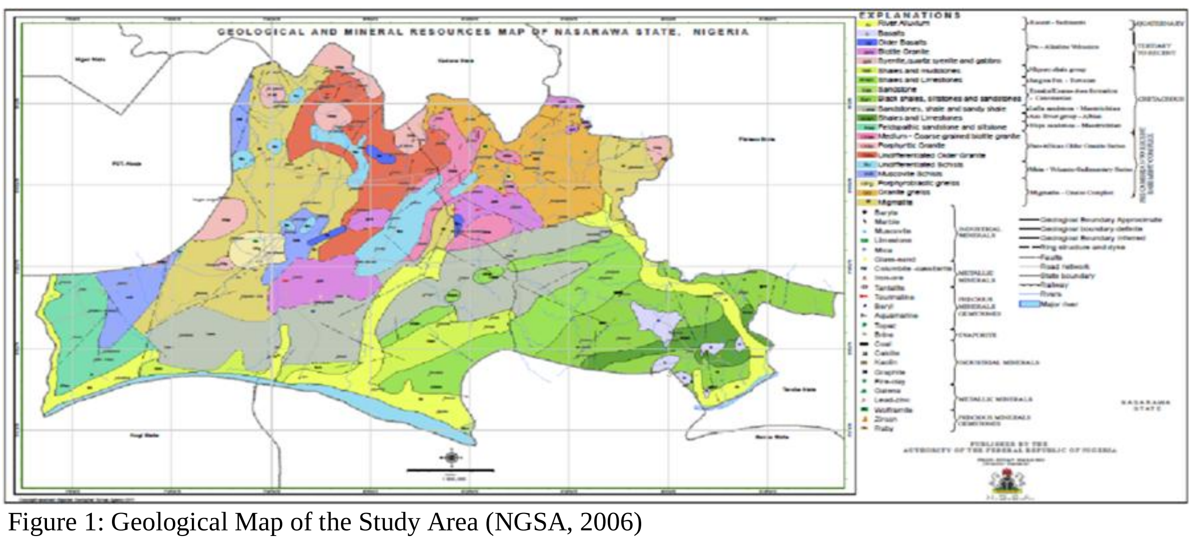

Figure 1: Geological Map of the Study Area (NGSA, 2006)

MATERIALS AND METHODS

Data Acquisition

Data Acquisition Aeromagnetic and airborne radiometric data over the study area were obtained from the Nigeria Geological Survey Agency (NGSA). The data were acquired during the nationwide airborne geophysical survey carried out by Fugro Airborne Surveys from December 2006 to May 2007. Survey parameters are shown in Table 1.

Table 1: Airborne Geophysical Survey Specifications and Parameters

Parameter	Specification
Aircraft	Cessna Caravan 208B, Cessna 406
Magnetic Sensor	Scintrex CS3 Cesium Vapour Magnetometer
Flight Line Spacing	500 metres
Tie Line Spacing	5 kilometres
Flight Direction	NW–SE
Terrain	Clearance 80 m
Sampling Interval	1 second (~75 metres)
Radiometric Sensor Gamma-ray	Spectrometer (1Hz sampling)

Aeromagnetic Data Processing

Data processing was performed using Geosoft Oasis Montaj 8.4 software. The following processing steps were applied:

Gridding

The randomly scattered survey data were gridded on a uniform grid using the minimum curvature gridding method. The grid cell size was 200 x 200 m.

Reduction to Equator (RTE)

The Equator correction was applied to reduce the effects of low magnetic latitude and to place the anomalies over their sources. The parameters were geomagnetic inclination = -6.68°; geomagnetic declination = -28.55°; amplitude correction inclination = 20°. RTE was preferred to RTP (Reduction to Pole) because of the instability of the latter at low latitudes, which can cause artefacts (Beard et al., 2000).

Regional-Residual Separation

The TMI grid was upward continued to 500 m to get the regional field. The residual magnetic intensity grid was generated by subtracting the upward continued data from the original TMI grid.

Enhanced Magnetic Products

The residual magnetic data were processed by the following enhancement techniques:

Analytic Signal (AS) The amplitude of analytic signal was calculated with the equation described by Roest et al. (1992):

$$A(x,y) = \sqrt{(\partial T/\partial x)^2 + (\partial T/\partial y)^2 + (\partial T/\partial z)^2} \quad (1)$$

The analytic signal is independent of the direction of the magnetisation, so it is capable of detecting edges at all magnetic latitudes (Nabighian, 1972; MacLeod et al., 1993).

The first vertical derivative was calculated using Fourier transform in the wavenumber domain. The FVD is a method that enhances shallow magnetic sources and emphasises minor structural anomalies (Milligan & Gunn, 1997; Foss, 2011).

Tilt Derivative (TDR): The tilt derivative was calculated using (Miller & Singh, 1994):

$$TDR = \tan^{-1}\left(\partial T/\partial z \div \sqrt{(\partial T/\partial x)^2 + (\partial T/\partial y)^2}\right) \quad (2)$$

The TDR is an automatic gain control filter that equalises responses of weak and strong anomalies (Verduzco et al., 2004).

Radiometric Data Processing

Radioelement Concentration Maps

Maps of potassium (K), thorium (Th) and uranium (U) concentration were created using the Grid and Image tool in Geosoft Oasis Montaj. The data were analysed using mini-curvature gridding to produce continuous images of radioelement dispersion.

Ratio Maps

Th/K, Th/U and K/U ratio maps were generated to enhance relative radioelement variations and assist lithological and regolith interpretation (Dickson & Scott, 1997; Wilford et al., 1997; IAEA, 2003). Ratio anomalies were interpreted cautiously because surface conditions can affect individual radioelement responses.

Ternary Radiometric Image

A three-way RGB colour model was created, with potassium as red, thorium as green and uranium as blue. The uranium channel was coloured blue because its low signal-to-noise ratio makes it less visible in the final image. The resulting images are coloured according to the relative intensities of the three elements, with subtle variations in the relative ratios of the three bands.

Lithological Interpretation

Lithological interpretation was based on the combined spatial relationships among the RTE/RMI, AS, FVD and TDR magnetic products, K, Th and U concentration maps, ratio maps, the ternary image and the existing geological map in ArcGIS 10.7. High magnetic responses were treated as indicators of rocks or structures containing relatively magnetic minerals, whereas lower responses may occur over felsic, weathered or sedimentary domains. Elevated K was used as supporting evidence for K-bearing felsic lithologies, while Th and U patterns were interpreted as relative radioelement responses influenced by source lithology and near-surface materials. No single magnetic or radiometric response was used as a unique lithological diagnostic;

units were inferred where multiple datasets showed consistent spatial patterns.

RESULTS AND DISCUSSION

Aeromagnetic Results

Total Magnetic Intensity (TMI) Map

The TMI map (Figure 2) shows a broad spatial contrast between the basement-dominated northern and southeastern parts of the study area and the sedimentary terrain in the south. The basement and mafic volcanic domains are characterised by relatively higher magnetic responses, whereas the sedimentary terrain is dominated by lower responses. The central part represents a transition between the magnetic basement and the sedimentary cover. These regional contrasts are consistent with previous aeromagnetic investigations in Nasarawa State, which similarly identified higher magnetic signatures over basement terrains and lower signatures over sedimentary areas (Adewumi and Salako, 2018). Because the present manuscript does not report the minimum and maximum values read from the TMI grid, the interpretation is expressed qualitatively rather than introducing unsupported numerical ranges.

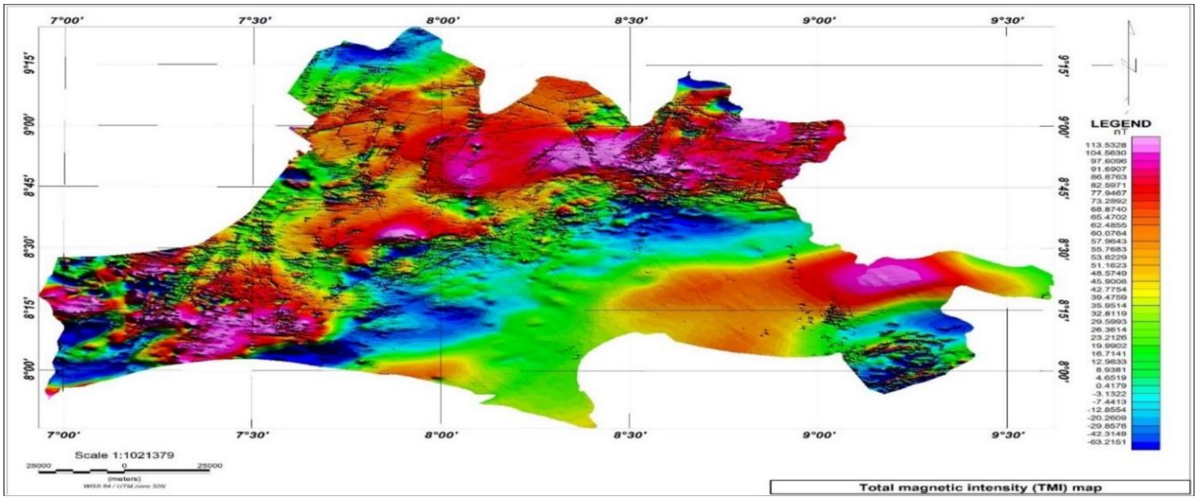

Figure 2: Total Magnetic Intensity (TMI) Map of the Study Area

Residual Magnetic Intensity (RMI) Map

The RMI map (Figure 3) reveals detailed magnetic anomalies that were not evident on the TMI map. Several high, low, and intermediate magnetic anomalous zones are delineated in Table 2.

Table 2: Interpretation of Magnetic Anomalies

Zone	Location	Interpretation
High Magnetic Anomalies (HM)	Southwestern parts	Duricrust and ferruginized sandstone of Bida Formation
High Magnetic Anomalies (HM)	Southeastern parts	Carbonaceous shales and mafic volcanics, Awe Formation
Circular/Sub-circular Features (G1-G4)	Nasarawa Udegi, Eggon Hills, Wamba	Granitic alkaline intrusives
Short Wavelength Anomalies (OG)	Various locations	Undifferentiated Older Granite and Gneiss Suite
Low Magnetic Lows (LM)	Southern and central parts	Sedimentary terrain (Bida, Lafia, Keana/Awe Formations)

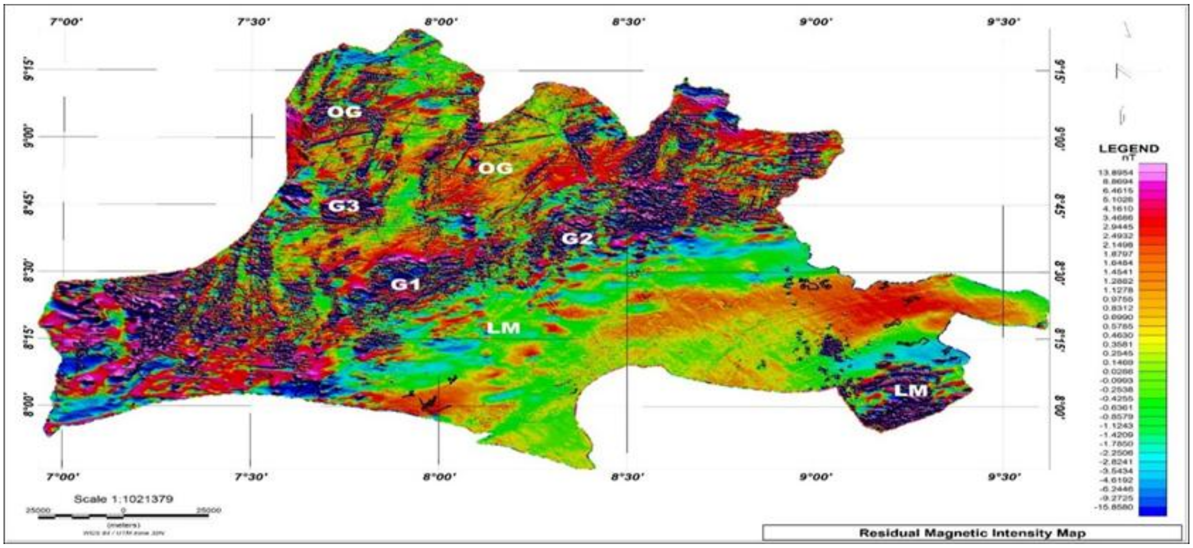

Figure 3: Residual Magnetic Intensity (RMI) Map of the Study Area

These interpretations are consistent with the use of aeromagnetic anomalies for distinguishing basement domains, intrusive bodies and structural features in north-central Nigeria (Adewumi and Salako, 2018).

Analytic Signal (AS) Map

The AS map (Figure 4) enhances the gradients around magnetic sources and therefore provides clearer expression of contacts and boundaries. The map highlights the southwestern magnetic anomalies associated with the Bida Formation, the southeastern anomalies associated with the Awe Formation and the circular to sub-circular anomalies interpreted as granitoid bodies in the Nasarawa Udegi, Eggon Hills and Wamba areas. The distribution of these anomalies provides an independent magnetic expression of the major lithological contrasts identified from the RMI map and supports the interpretation of intrusive contacts and basement boundaries.

Figure 4 shows that the AS map clearly delineated the peripheries of magnetic entities and geological boundaries. Duricrust and ferruginous sandstone of the Bida Formation are associated with southwestern magnetic anomalies. The magnetic anomalies in the southeast correlate with carbon-rich shales and mafic volcanic rocks of the Awe Formation. The circular features (G1, G2, G3, G4) are distinctly identified as granitic intrusions in the Nasarawa Udegi, Eggon Hills and Wamba areas. The OG regions exhibit intercalations of high, moderate and low formations in agreement with the undifferentiated Older Granite Suite.

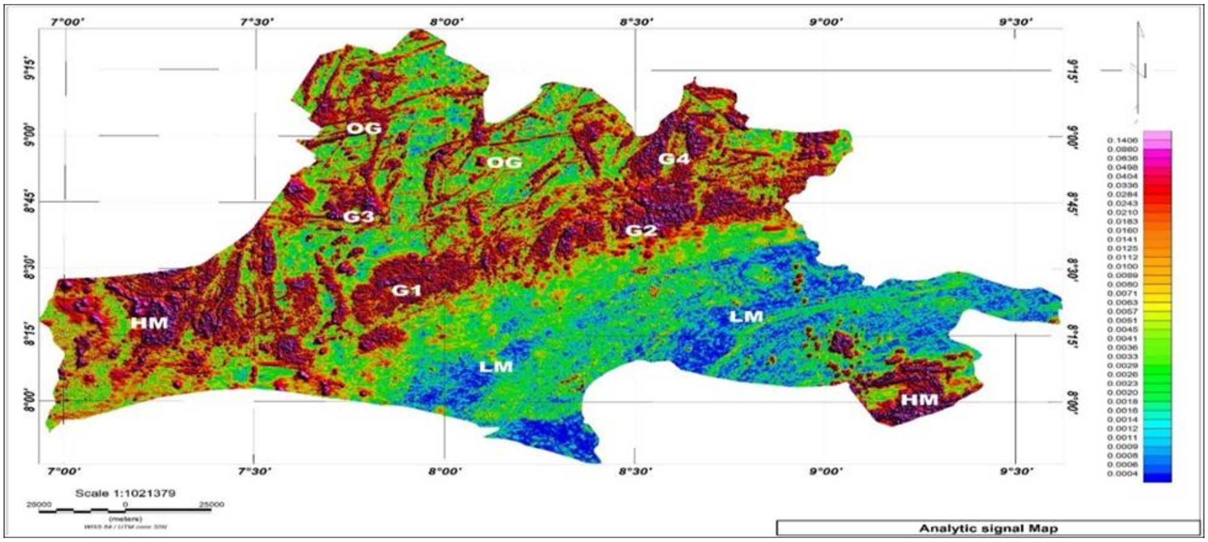

Figure 4: Analytic Signal (AS) Map of the Study Area

Radiometric Results

Potassium (K) Concentration Map

The potassium concentration map (Figure 5) reveals significant variations in potassium distribution across the study area. Low potassium concentration is observed at the southern and central parts, coinciding with the sedimentary terrain (Bida Formation to the extreme southwest, Lafia Formation and parts of Keana/Awe Formation at the central parts). This observation is consistent with the general loss of K during pedogenesis, where K concentration decreases with increasing weathering because K is highly soluble under most weathering environments and is rapidly leached. High potassium concentration is observed at the northern parts (basement terrain) and southeastern parts (mafic volcanics and carbonaceous shales of the Awe Formation) and at two circular features observed on the magnetic maps (labeled G1 and G2 corresponding to granitic alkaline intrusives). The elevated K in these areas is attributed to the presence of K-feldspar and mica-rich lithologies.

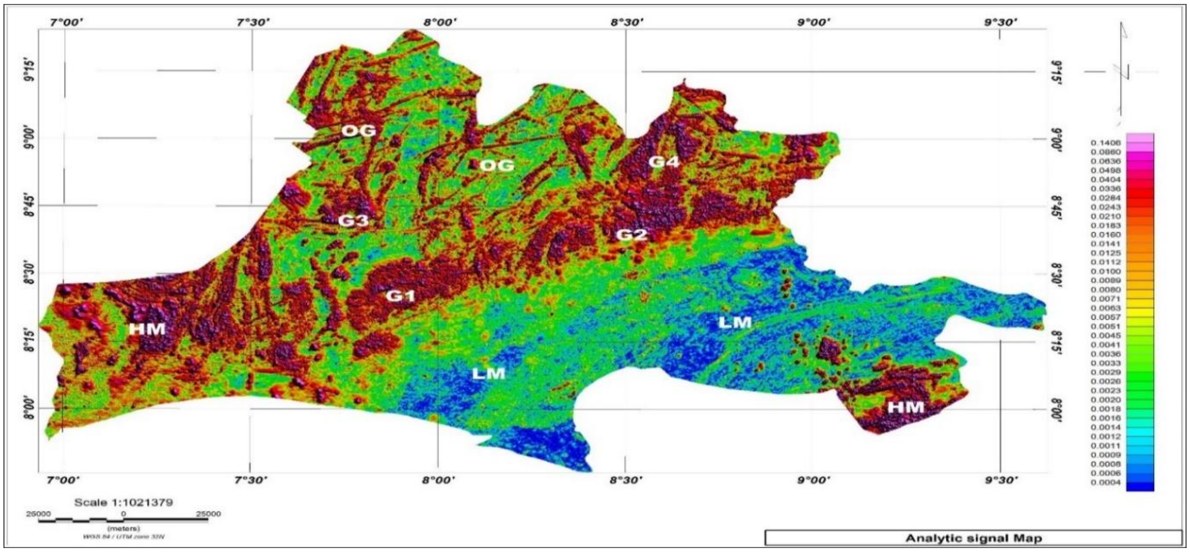

Figure 5: Potassium (K) Concentration Map of the Study Area

Uranium (U) Concentration Map

The uranium concentration map (Figure 6) shows relatively elevated responses around the circular features G1–G3 and in parts of the north-central, southeastern and southwestern domains, while lower responses occur across much of the central and southern areas. Unlike the K and Th maps, the U distribution does not consistently delineate lithological boundaries. Short-wavelength streaks are also evident and may reflect the sensitivity of airborne uranium measurements to environmental and atmospheric effects, including radon. Consequently, uranium anomalies are interpreted as supporting evidence rather than as standalone indicators of lithology or hydrothermal alteration.

Figure 6, the uranium concentration map, shows high uranium values associated with circular features on magnetic maps designated G1, G2 and G3. These round formations can be seen in the Th and K maps. They can also be seen in the uranium map. High levels of uranium are also found in the north-central, southeastern and southwestern areas. The mafic volcanic rocks and shales of the Awe Formation correspond to the south east region. Concentration is reduced in the Central Regions and the southernmost area adjoining Benue State, corresponding to the Benue River.

Uranium distribution is affected by topography and slope. In low-relief areas, where water movement is subdued, stream sediments show a higher percentage of finer particles that are more favourable for longer dispersion paths of uranium. Thus, uranium concentrations are generally low in the western part of the study area, with high relief, except for the two circular features identified as granitic rocks.

The uranium map was not able to distinctly delineate the boundaries of the different lithologies of the region. The image shows short wavelength anomalies that are associated with noise due to fluctuations of the atmospheric radon levels during the survey and result in strong streaking in the image. It is a common feature in uranium imagery (Minty, 1997) and is independent of processing applied to the dataset.

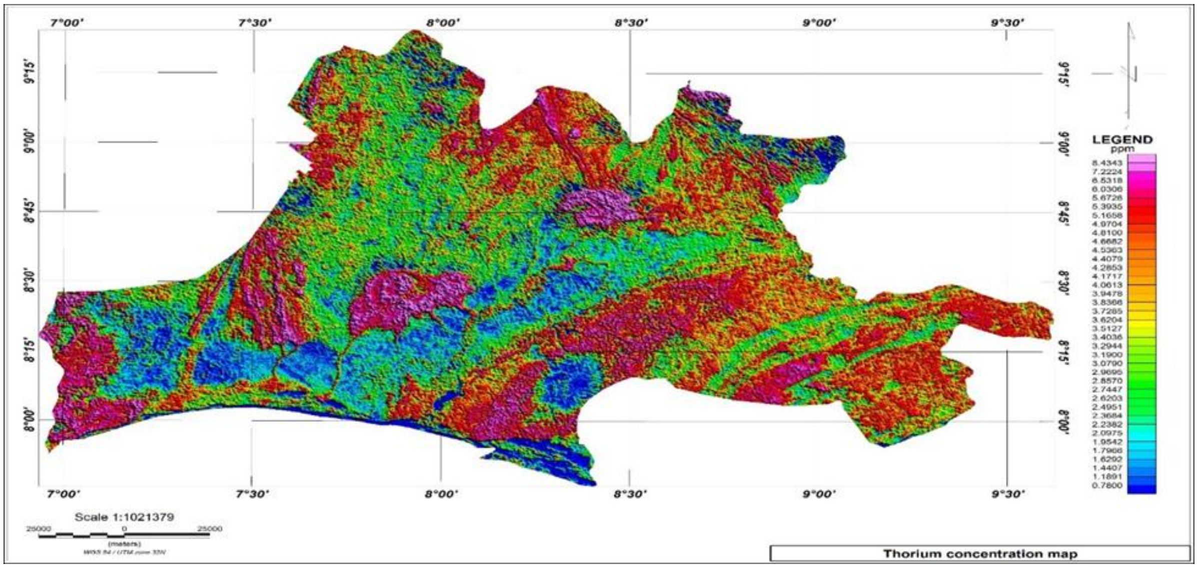

Figure 6: Uranium (U) Concentration Map of the Study Area

Thorium (Th) Concentration Map

The thorium concentration map (Figure 7) is useful for delineating the lithology and lithological boundaries of the region. High Th concentrations are concentrated in the southeast, northeast and southwest and low concentrations in the central parts, with the exception of the circular features identified on the K and U maps as felsic granitic bodies. The high levels of Th found at these sites can be explained by the high temperatures involved in the formation of these geological structures. The phases formed at higher temperatures seem to contain the maximum amount of the substance. Weathering releases thorium that can be stored in iron or titanium oxide-hydroxides and clays (Martelet et al., 2006).

Thorium is generally considered as highly immobile and insoluble and generally remains with its parent rock or is transported over limited distances. Thus low thorium areas are indicative of remobilisation of thorium during the incursion of hydrothermal fluids. K vs. Th opposition means simultaneous decrease of Th when K increases with modification (Ostrovskiy, 1975). This allowed the areas to be modified to be identified.

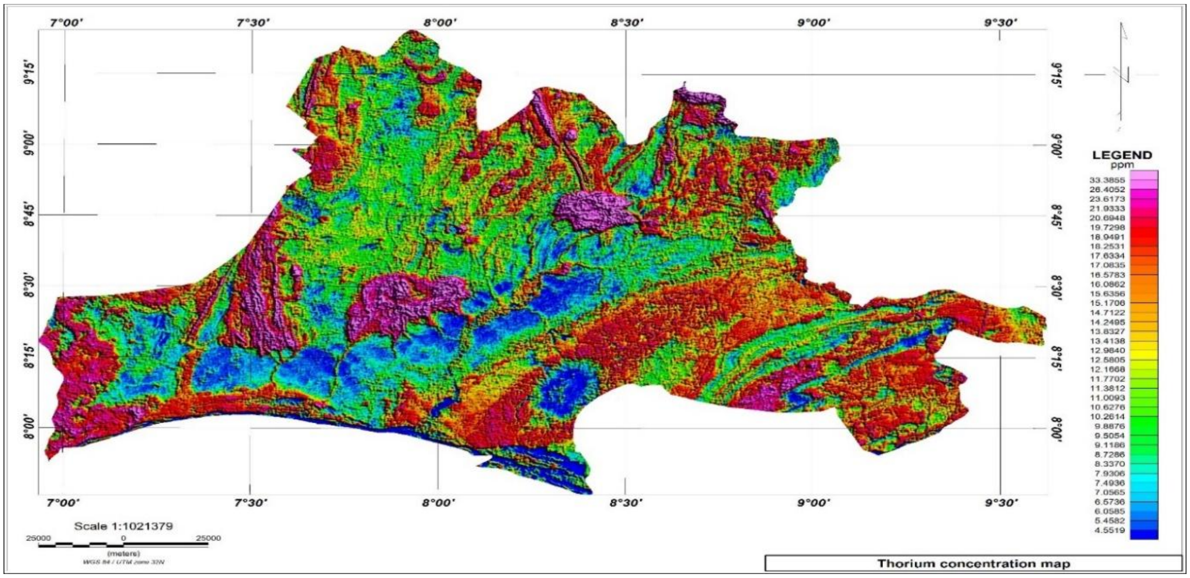

Figure 7: Thorium (Th) Concentration Map of the Study Area

Ratio Maps

The Th/K, Th/U and K/U ratio maps (Figures 8–10) were used to enhance relative radioelement variations and reduce some common effects affecting individual element maps. Low Th/K values may indicate relative K enrichment, whereas high Th/U values may reflect relative U depletion and low Th/U values may indicate relative U enrichment. Elevated K/U values indicate relative K enrichment. These ratios are useful for identifying areas that warrant investigation for alteration or regolith modification, but they are not sufficient by themselves to prove hydrothermal alteration. In this study, ratio anomalies were therefore considered together with the magnetic responses, ternary image and existing geological map.

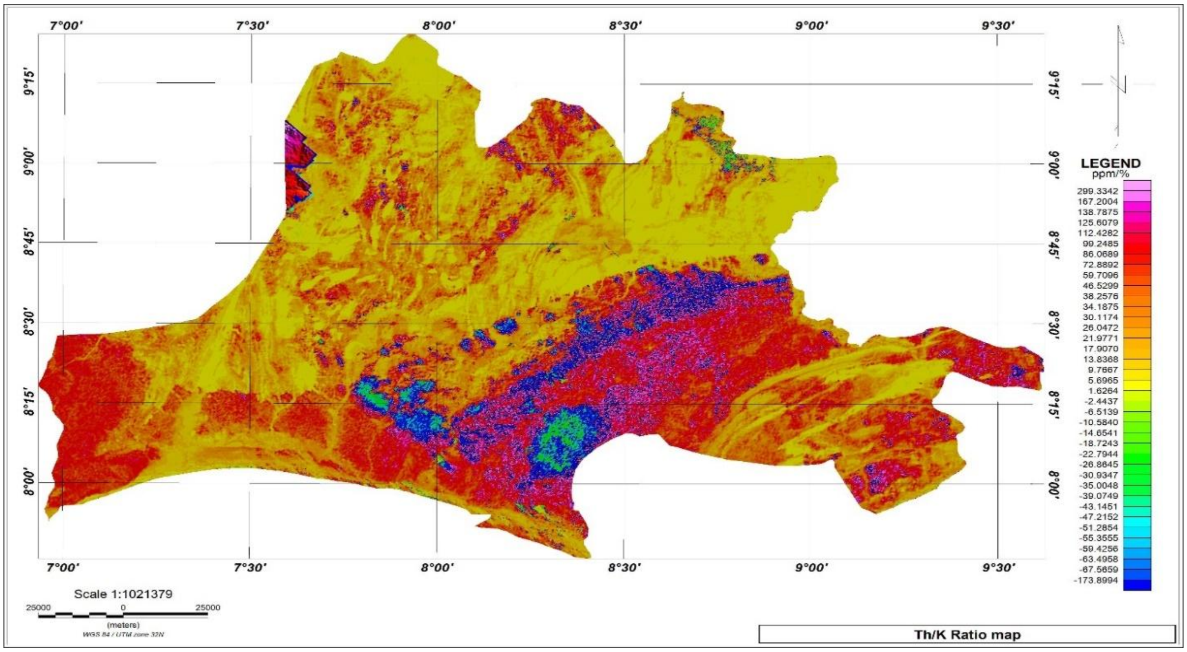

Figure 8: Th/K Ratio Map of the Study Area

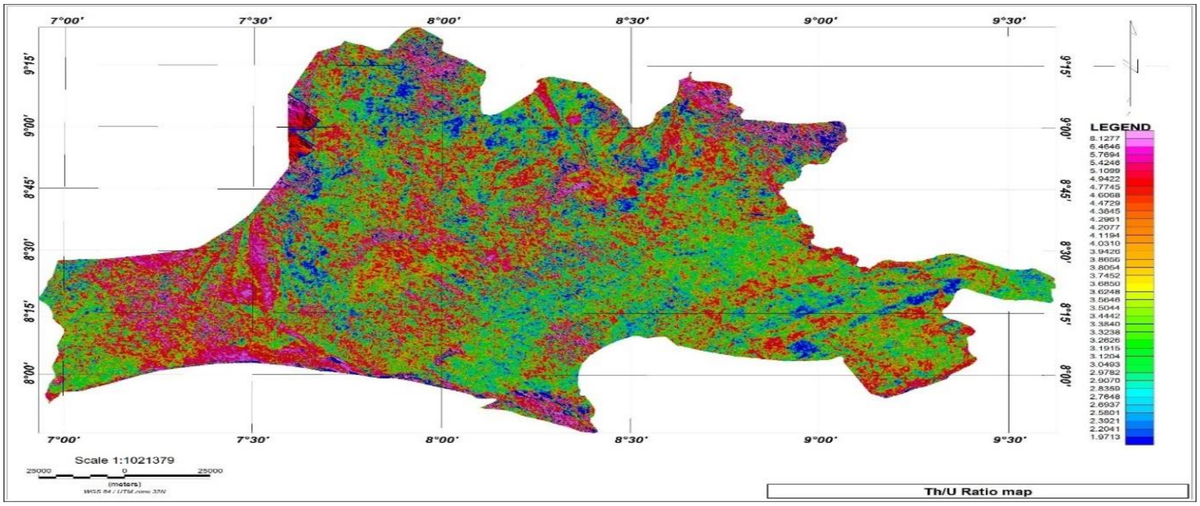

Figure 9: Th/U Ratio Map of the Study Area

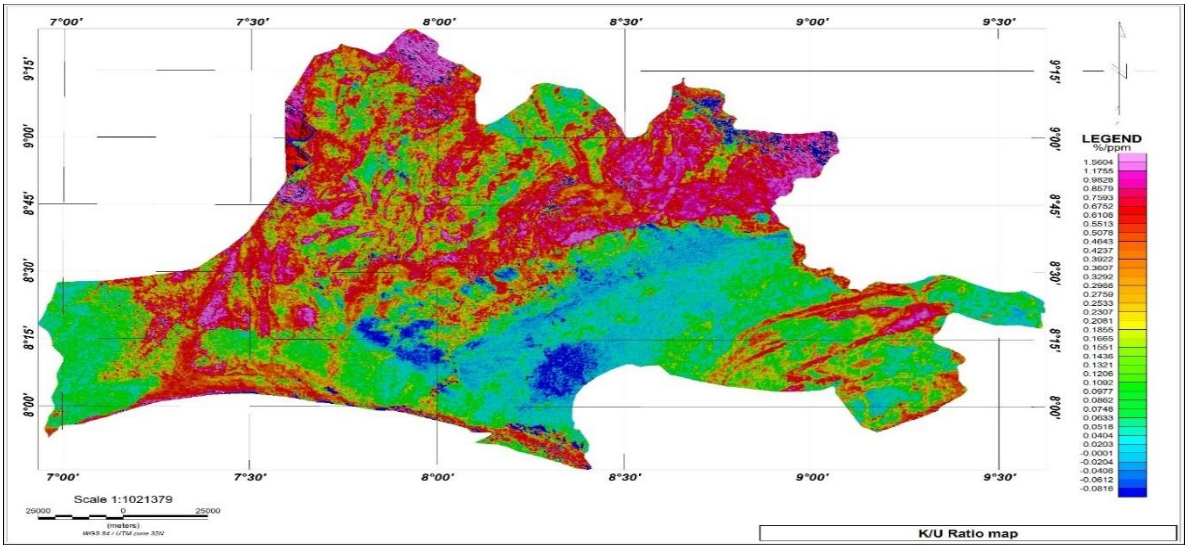

Figure 10: K/U Ratio Map of the Study Area

Ternary Radiometric Image

The ternary radiometric image (Figure 11) integrates the relative distributions of K, Th and U. Red to yellow domains represent relatively higher K and/or Th contributions and are concentrated around felsic intrusive and pegmatitic areas, whereas darker domains generally correspond to lower total radioelement responses. Green and blue components represent relative contributions from Th/U and U, respectively. The ternary image broadly agrees with the mapped geological framework and is particularly useful when interpreted jointly with the magnetic maps. The colour classes should be regarded as relative radiometric signatures rather than unique lithological labels because surface conditions and regolith can modify airborne gamma-ray responses.

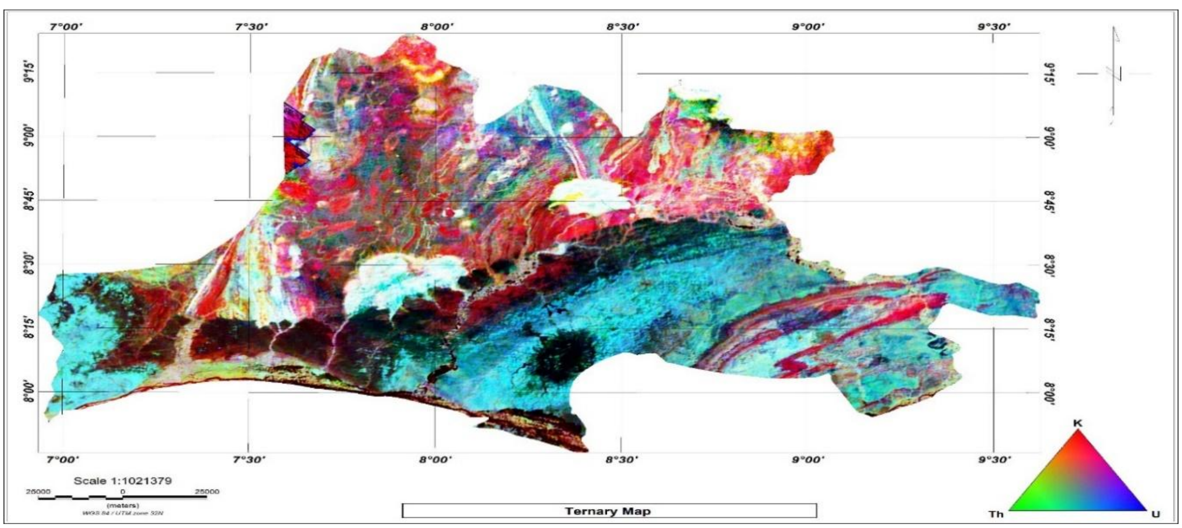

Figure 11: Ternary Radiometric Image of the Study Area

Integrated Lithological Interpretation

Integration of the RTE/RMI, AS, FVD and TDR products with K, Th, U, ratio and ternary radiometric maps provides the basis for distinguishing the principal lithological domains. The strongest interpretation is obtained where independent magnetic and radiometric responses coincide. The migmatite-gneiss complex is characterised by moderate to high magnetic responses and generally low to moderate radioelement responses; schist belts display variable magnetic and radiometric signatures; granitoids and interpreted Younger Granite bodies generally show lower to moderate magnetic responses with relatively elevated radioelements; pegmatites are expressed by low magnetic and relatively high K responses; mafic intrusive rocks show stronger magnetic responses with comparatively low radioelement responses; and the sedimentary formations are dominated by lower magnetic responses with generally low K and moderate relative Th and U responses. These relationships are summarised in Table 3 and form the basis for the lithological map.

Table 3: Integrated Lithological Interpretation

Lithological Unit	Magnetic Response	Radiometric Response	Ternary Colour	Interpretation
Migmatite-Gneiss Complex	Moderate-High	Low-Moderate K, Th, U	Green-Black	Heterogeneous basement
Schist Belts	Variable	Variable K, Th, U	Various	Metasedimentary/Metavolcanic
Older Granites	Moderate-Low	High K, Th, U	Red-Yellow	Pan-African granitoids
Younger Granites	Moderate-Low	High K, Th, U	Red-Yellow	Jurassic intrusives
Pegmatites	Low	High K	Red	Fractionated granitic melts
Mafic Intrusives	High	Low K, Th, U	Green	Gabbro, dolerite
Bida Formation	Low	Low K, Moderate Th, U	Dark	Sandstone, laterite
Lafia Formation	Low	Low K, Moderate Th, U	Dark	Shale, sandstone
Keana/Awe Formation	Low-Moderate	Low K, Moderate Th, U	Dark-Green	Carbonaceous shales, mafic volcanics

Lithological Unit Descriptions

Migmatite-Gneiss Complex

The migmatite-gneiss assemblage has moderate to high magnetic intensity with generally low to moderate concentrations of radioelements. The magnetic signature is diverse and reflects variations in mineralogy, in deformation intensity and in metamorphic grade. These rocks make up a significant proportion of the Basement Complex and define the regional structure within which the younger lithologies have been intruded. Magnetite-rich layers and highly altered basement areas in the gneiss terrain are known to correspond to regions of increased magnetic activity.

The radiometric profile of the migmatite-gneiss complex is variable with potassium low to moderate, thorium generally low and uranium low. The ternary image presents a colour gradient from green to black, indicating low relative concentrations of radioelements compared with felsic intrusive rocks.

Schist Belts

The schist belts are characterised by large radiometric variability, which reflects variations in protolith composition, metamorphic setting and degree of alteration. Within the schistose landscape, three main radiometric zones were identified:

i. Domain 1: Intermediate levels of thorium with low concentrations of potassium and uranium.
ii. Domain 2: Higher thorium and uranium concentrations, and relatively low potassium concentrations, indicate enrichment of durable accessory minerals during metamorphic and weathering processes.
iii. Domain 3: Generally low values for all three radioelements.

These variations indicate a high compositional diversity of the schist belts and reflect the complex tectono-metamorphic evolution of the studied region.

Granitic Rocks and Younger Granite Intrusions

Granitic formations and Younger Granite intrusions are characterised by high levels of potassium, thorium, and uranium along with comparatively low to moderate magnetic signatures. These rocks usually appear as sub-circular to elliptical radiometric anomalies and are intrusive bodies emplaced during different magmatic events. The high concentration of radioelements points to a felsic composition and accumulation of incompatible elements during magmatic differentiation.

These units appear in the ternary image as a gradient of red to yellow, reflecting higher levels of potassium and thorium relative to uranium. Variations in radioelement concentrations in some granitoid types are related to hydrothermal alteration, weathering, mineralisation and magmatic fractionation.

Many granitic bodies have been extensively altered by hydrothermal alteration, destroying their original geochemical signatures. Potassic alteration is usually characterised by an increase in potassium associated with the formation of secondary K-feldspar and sericite. Thorium can be depleted during potassic alteration. Uranium is highly mobile in oxidising conditions can be leached from the source rocks and then re-precipitated in structurally controlled environments or in sedimentary environments. Thorium is relatively immobile and normally remains close to the source. Therefore, thorium concentration patterns are important indicators of primary lithological boundaries.

Pegmatites

Radiometric maps show pegmatites have low magnetic responses and high potassium. These characteristics are manifested as linear to sub-circular irregularities associated with major shear zones and granitic intrusions. High potassium values reflect the abundance of K-feldspar and mica in these differentiated granitic melts. There are also several occurrences of pegmatite in the Wamba, Eggon and Udegi areas. The lithium bearing pegmatite types are associated with the largest potassium anomalies.

Mafic and Intermediate Intrusive Rocks

Mafic and intermediate intrusive rocks have high magnetic intensity, and low concentrations of radioelements. This association is consistent with the presence of ferromagnesian minerals and magnetite in mafic lithologies and the generally low volume of potassium-bearing minerals and radioactive accessory phases. The strong magnetic signatures associated with these rocks are an important contrast to the felsic intrusive and metamorphic rocks adjacent to them.

Sedimentary Formations

The sedimentary formations of the Benue Trough and related alluvial deposits are characterised by low potassium contents and moderate thorium and uranium concentrations. The lithologies are generally displayed as dark zones in the ternary radiometric image, with localised blue-green tones indicative of minor enrichment in uranium and thorium. The moderate concentrations of thorium and uranium are due to adsorption on clay minerals and co-precipitation with iron oxides during weathering and sedimentary processes. Potassium is highly mobile in weathering environments and is easily leached from sediments, leading to decreased potassium signatures compared to adjacent basement rocks.

The sedimentary landscape is of great importance as it occurs in depressions and drainage system that are structurally controlled formed around the Basement Complex and Younger Granite areas. These sediments have accumulated through geological epochs detrital material from weathering and erosion of nearby granitoids, pegmatites, gneisses and schists. Thus, secondary concentrations of valuable minerals such as cassiterite, columbite-tantalite, monazite, zircon, gold, and other heavy minerals derived from primary source rocks may be present in the stream channels, floodplains, and alluvial deposits.

Lithological Boundaries

The integrated datasets delineate several major lithological boundaries (Table 4). The basement–sediment contact is expressed by a marked magnetic contrast accompanied by changes in the K and Th responses. Granite–gneiss contacts are associated with circular to elliptical magnetic features and transitions in ternary radiometric response. Schist–gneiss boundaries are characterised by moderate magnetic contrasts and variable radioelement responses, while mafic–felsic intrusive contacts are expressed by strong magnetic contrasts accompanied by changes in K, Th and U. Because these boundaries are geophysical interpretations, they should be regarded as inferred contacts pending detailed field verification.

Table 4: Key Lithological Boundaries

Boundary	Location	Magnetic Expression	Radiometric Expression
Basement-Sediment	Northern-southern transition	Sharp magnetic contrast	Sharp K/Th contrast
Granite-Gneiss	Various intrusive contacts	Circular to elliptical anomalies	Red-yellow to green transition
Schist-Gneiss	Schist belt margins	Moderate magnetic contrast	Variable radioelement contrast
Mafic-Felsic	Intrusive contacts	High-low magnetic contrast	Low-high K, Th, U contrast

Relationship Between Lithology and Mineralization

The integrated interpretation identifies lithological settings that are favourable for further mineral exploration, rather than proving mineralisation directly. The sedimentary sequences of the Middle Benue Trough, particularly the Keana/Awe Formation, are associated with documented Pb–Zn–baryte occurrences. In the Basement Complex, the Wamba, Eggon and Udegi areas contain documented pegmatitic and granitic mineral occurrences, and the associated elevated K responses provide useful exploration indicators. Columbite–tantalite and gemstone occurrences are commonly associated with pegmatitic and granitic environments, while gold occurrences are associated with basement rocks and structurally complex zones. The present geophysical results therefore help define lithological and structural environments for follow-up exploration, but the airborne anomalies alone cannot establish the grade or economic significance of mineralisation.

Comparison with Previous Studies

The present interpretation is broadly consistent with earlier geological and aeromagnetic studies of Nasarawa State. Adewumi and Salako (2018) reported higher magnetic responses over basement terrains around Wamba, Akwanga and Nasarawa Eggon and lower responses over the southern sedimentary terrain. Previous work in the Wamba and adjoining areas also recognised basement complex rocks, Younger Granites and Cretaceous sedimentary rocks, with structural trends that can be detected using aeromagnetic data. The present study extends this interpretation by integrating magnetic products with airborne K, Th and U responses and ternary radiometric imagery. The agreement between the datasets strengthens the interpretation of the principal lithological domains, although field mapping remains necessary for confirmation.

Table 5: Comparison with Previous Studies

Study	Area	Lithological Units	Methodology
This Study	Nasarawa State	Migmatite-Gneiss, Schist, Granite, Pegmatite, Sedimentary	Integrated Magnetic + Radiometric
Obaje (2009)	Nigeria	Basement Complex, Younger Granites, Sedimentary Basins	Geological Mapping
NGSA (2006)	Nasarawa State	Basement Complex, Benue Trough	Geological Mapping
Rahaman (1988)	Nigerian Basement	Migmatite-Gneiss, Schist, Granite	Geological Mapping

CONCLUSION

The integrated aeromagnetic and airborne radiometric interpretation delineated the principal lithological domains of Nasarawa State, including the migmatite-gneiss complex, schist belts, granitoids, pegmatites, mafic to intermediate intrusive rocks and sedimentary formations of the Middle Benue Trough. The magnetic products, particularly RMI and AS, enhanced lithological contrasts, intrusive geometries and inferred contacts, while the K, Th, U, ratio and ternary products provided complementary information for radiometric discrimination. The combined interpretation indicates that the basement and mafic domains generally have stronger magnetic responses, whereas granitoid and pegmatitic domains are associated with relatively elevated K and other radioelements. The sedimentary terrain is generally characterised by lower magnetic responses and lower K with moderate relative Th and U responses. The study area covers approximately 27,000 km², and the survey was acquired at 500 m flight-line spacing with a 200 × 200 m processing grid. The integrated results provide a regional lithological framework and identify areas suitable for detailed geological, geochemical and ground-geophysical follow-up.

LIMITATIONS AND UNCERTAINTIES

The following limitations are acknowledged:

i. Data Resolution: The 500 m line spacing limits the detection of small-scale lithological variations (< 500 m length).
ii. Weathering Effects: Intense weathering in tropical environments may mask primary radiometric signatures.
iii. Vegetation Cover: Dense vegetation may attenuate radiometric signals.
iv. Soil Thickness: Thick soil cover may obscure bedrock signatures.
v. Sedimentary Cover: Thick sedimentary cover may obscure basement lithologies.

RECOMMENDATIONS

i. Geological mapping: Checking the inferred lithological boundaries by means of detailed geological mapping.
ii. Geochemical Assessments: Lithological interpretations were supported by the collection of soil and stream sediment samples, which were also used to identify geochemical anomalies.
iii. Ground geophysics: Carry out magnetic and radiometric surveys in priority target areas to improve lithological mapping.
iv. Investigative drilling to verify lithological evaluations and assess potential mineralisation.
v. Complete GIS Database: Integration of lithological data with structural, geochemical and remote sensing data for better targeting.

SIGNIFICANCE

The research demonstrates that the integration of aeromagnetic and airborne radiometric data provides an efficient and cost-effective means for conducting regional lithological mapping, particularly in regions characterised by limited bedrock exposure, complex basement geology, and intense weathering. The lithological map produced provides a good base for mineral exploration targeting especially in structurally controlled granitoid terrains, schist belts, pegmatite zones and sedimentary environments that may host secondary mineral deposits. The techniques used in this study can be applied to other parts of the Nigerian Basement Complex and similar geological settings in West Africa.

ACKNOWLEDGEMENT
The authors wish to thank Nigeria Geological Survey Agency (NGSA), Abuja for the provision of the aeromagnetic and airborne radiometric data used for this research. The authors gratefully acknowledge Nasarawa State University, Keffi for the facilities and a good environment for this study. The authors acknowledge the academic and technical staff of the Department of Geology for their valuable comments and suggestions that greatly improved the quality of this manuscript. The authors acknowledge with gratitude all the colleagues and reviewers who contributed to the advancement and perfection of this work.

REFERENCES
Adewumi, T. and Salako, K. A. (2018). Delineation of mineral potential zone using high resolution aeromagnetic data over part of Nasarawa State, North Central Nigeria. Egyptian Journal of Petroleum, 27(4), 759–767. https://doi.org/10.1016/j.ejpe.2017.11.002

Beard, L. P., Kaiser, K. and Taylor, S. (2000). Reduction to the equator of low-latitude magnetic anomalies. Geophysics, 65(3), 812-821.

Dada, S. S. (2006). Proterozoic evolution of Nigeria. In: Oshi, O. (ed.) The Basement Complex of Nigeria and its Mineral Resources. Akin Jinad & Co., Ibadan, pp. 29-44.

Dickson, B. L. and Scott, K. M. (1997). Interpretation of aerial gamma-ray surveys—adding the geochemical factors. AGSO Journal of Australian Geology and Geophysics, 17(2), 187-200.

Fatoye, F. B., Ibitomi, M. A. and Omada, J. I. (2014). Lead-zinc-barytes mineralization in the Benue Trough, Nigeria: Their geology, occurrences and economic prospective. Advances in Applied Science Research, 5(1), 102-110.

Foss, C. (2011). Magnetic data enhancement and depth estimation. In: Gupta, H. (ed.) Encyclopedia of Earth Sciences Series. Springer, pp. 736-746.

Gunn, P. J. (1997). Regional magnetic and radiometric surveys for geological mapping. AGSO Journal of Australian Geology & Geophysics, 17(2), 63-73.

Gunn, P., Minty, B. and Milligan, P. (1997). The airborne gamma-ray spectrometric response over arid Australian terranes. In: Gubins, A. (ed.) Proceedings of Exploration 97: Fourth Decennial International Conference on Mineral Exploration. Australia, pp. 733-740.

IAEA (International Atomic Energy Agency). (2003). Guidelines for radioelement mapping using gamma-ray spectrometry data. IAEA-TECDOC-1363. Vienna.

MacLeod, I. N., Jones, K. and Dai, T. F. (1993). 3-D analytic signal in the interpretation of total magnetic field data at low magnetic latitudes. Exploration Geophysics, 24, 679–688. https://doi.org/10.1071/EG993679

Martelet, G., Truffert, C., Tourlière, B., Ledru, P. and Perrin, J. (2006). Classifying airborne radiometry data with agglomerative hierarchical clustering: A tool for geological mapping in context of rainforest (French Guiana). International Journal of Applied Earth Observation and Geoinformation, 8(3), 208-223.

Miller, H. and Singh, V. (1994). Potential field tilt—a new concept for location of potential field sources. Journal of Applied Geophysics, 32, 213–217. https://doi.org/10.1016/0926-9851(94)90022-1

Milligan, P. R. and Gunn, P. J. (1997). Enhancement and presentation of airborne geophysical data. AGSO Journal of Australian Geology and Geophysics, 17(2), 63-75.

Minty, B. (1997). Fundamentals of airborne gamma-ray spectrometry. AGSO Journal of Australian Geology & Geophysics, 17(2), 39-50.

Nabighian, M. N. (1972). The analytical signal of two-dimensional magnetic bodies with polygonal cross-section: Its properties and use for automated anomaly interpretation. Geophysics, 37(3), 507-517.

NGSA (Nigeria Geological Survey Agency). (2006). The geological and mineral resource map of Nigeria (1:500,000). NGSA, Abuja.

Obaje, N. G. (2009). Geology and mineral resources of Nigeria. Springer, Heidelberg.

Ostrovskiy, E. (1975). Antagonism of radioactive elements in wallrock alteration fields and its use in aerogamma spectrometric prospecting. International Geology Review, 17(4), 461-468.

Rahaman, M. A. (1988). Recent advances in the study of the basement complex of Nigeria. In: Precambrian Geology of Nigeria. Geological Survey of Nigeria.

Reeves, C. (2005). Aeromagnetic surveys: Principles, practice and interpretation. Geosoft.

Roest, W., Verhoef, J. and Pilkington, M. (1992). Magnetic interpretation using 3-D analytical signal.

Geophysics, 57(1), 116–125. https://doi.org/10.1190/1.1443174

Shives, R., Charbonneau, B. and Ford, K. (2000). The detection of potassic alteration by gamma-ray spectrometry—recognition of alteration related to mineralization. Geophysics, 65(6), 2001–2011. https://doi.org/10.1190/1.1444883

Verduzco, B., Fairhead, J., Green, C. and Mackenzie, C. (2004). New insights into magnetic derivatives for structural mapping. The Leading Edge, 23, 116–119. https://doi.org/10.1190/1.1651454

Wilford, J., Bierwirth, P. and Craig, M. (1997). Application of airborne gamma-ray spectrometry in soil or regolith mapping and applied geomorphology. AGSO Journal of Australian Geology & Geophysics, 17(2), 201-216.

Black, R. (1980). Precambrian of West Africa. Episodes, 4, 3-8.